DOI: 10.1002/chem.200801182

Chlorinated Derivatives of C_{78}-Fullerene Isomers with Unusually Short Intermolecular Halogen–Halogen Contacts

Kalin S. Simeonov, Konstantin Yu. Amsharov, and Martin Jansen*[a]

Abstract: The chlorinated fullerenes $C_{78}(2)Cl_{18}$ and $C_{78}(3)Cl_{18}$ were synthesized by highly selective chlorination of the individual isomers. They were crystallized as $C_{78}(2)Cl_{18}{\cdot}Br_2{\cdot}TiCl_4$ and solvent free $C_{78}(3)Cl_{18}$. The carbon connectivities of both isomers have been confirmed through X-ray single-crystal analysis. Studious investigation of both crystal packings together with the crystal structure of $C_{78}(4)Cl_{18}$ has revealed the presence of unusually short intermolecular halogen–halogen contacts, which provide evidence for attractive intermolecular interactions, the nature of which is discussed.

Keywords: chlorination • fullerenes • intermolecular interactions • X-ray diffraction

Introduction

The existence of several structural isomers drastically complicates the investigation, as well as the structure determination of higher fullerenes. Although combining some restraints, such as the isolated pentagon rule (IPR), together with the presence of only five- and six-membered rings in the molecule, with NMR spectroscopic studies usually provides a confirmation of the constitution of fullerene species, a direct method of structure determination, such as X-ray crystallography, is envisaged to solve the query of a single-isomer recognition. The virtually spherical shape of all fullerenes and their rotational mobility in the crystal lattice define the poor quality of fullerene crystals. Up to date, except for C_{60} and C_{70}, no other ordered crystal structures of pristine fullerenes have been reported. Derivatization is an efficient approach to solving this problem.[1] In particular, halogenation has emerged as a powerful tool for obtaining well-crystallized C_{60} and C_{70} fullerene derivatives.[2] It was found that a mixture of Br_2 and $TiCl_4$ acts as a selective agent for the chlorination of C_{70} fullerene.[2e] Recently, we have successfully employed this mixture in an attempt to chlorinate C_{76} yielding $C_{76}Cl_{18}$, the first fully ordered crystal structure of a chiral fullerene.[3] The next recoverable from soot fullerene, C_{78}, has five IPR isomers.[4] Although separation techniques applicable to the soluble C_{78} isomers ($C_{78}(1)$, $C_{78}(2)$, and $C_{78}(3)$) are commonly available,[5,6] only two crystal structures including soluble C_{78} isomers as halogenated derivatives were reported thus far.[7] However, in these cases, different structural isomers occupy the fullerene site, which are presumably $C_{78}(2)$ and $C_{78}(3)$. The carbon connectivities of the nonsoluble $C_{78}(5)$ fullerene were crystallografically confirmed through analysis of $C_{78}(5)(CF_3)_{12}$.[8] The last elusive isomer $C_{78}(4)$ was recently discovered and characterized by our group.[9] Herein, we report the synthesis and single-crystal X-ray determination of $C_{78}(3)Cl_{18}$ (structure **I**) and $C_{78}(2)Cl_{18}$ (structure **II**), as well as the analysis of the fully ordered crystal of $C_{78}(4)Cl_{18}$ (structure **III**).[9] A detailed analysis of the crystal structures has clearly demonstrated the presence of numerous short Cl···Cl intermolecular contacts, the nature of which has long been a matter of interest and debate.[10–15]

The assumption that attractive interactions between halogen atoms should be considered was based on thorough analyses of crystal structures of halogenated hydrocarbons.[11] In this context, the halogen–halogen contacts in the crystal structures occurred preferably in two definite geometries, type **I** ($\theta_1 = \theta_2$) and type **II** ($\theta_1 = 180$, $\theta_2 = 90°$), in which θ_1 and θ_2 are the two C−Hal···Hal angles.[11] Type **I** contacts can be explained by the nonspherical shape of covalently bonded halogen atoms, which occupy a rather ellipsoidal volume in space.[12] As a consequence, the effective atomic radius of halogens along the extended C−Hal bond axis is

---

[a] K. S. Simeonov, Dr. K. Y. Amsharov, Prof. Dr. M. Jansen
Department of Chemistry
Max Planck Institute for Solid State Research
Heisenbergstrasse 1, 70569 Stuttgart (Germany)
Fax: (+49) 7116891502
E-mail: m.jansen@fkf.mpg.de

Supporting information for this article is available on the WWW under http://dx.doi.org/10.1002/chem.200801182.

smaller than the radius perpendicular to this axis. Previous analyses of high-quality crystal structures (excluding structures containing further heteroatoms, which can independently play a major role in determining the packing) have shown that short Cl···Cl distances of about 3.5 Å or even less in the case of head-to-head contacts ($\theta_1 = \theta_2 = 180°$) can be explained by close packing of anisotropic atoms.[13] In type **II** contacts, one halogen atom acts as a donor while the other acts as an acceptor. Such kinds of interaction between electronegative atoms (N, O, and S), which act as Lewis bases, and halogen atoms is well known as halogen bonding, by analogy with hydrogen bonding.[14] However, it was noted that "preferred orientations" are more typical for iodine atoms and are not obviously present to establish specific Cl···Cl interactions.[13] Moreover, quantum-chemical calculations have shown that Cl···Cl interactions can be classified as "nonbonding".[13]

The formation of short Cl···Cl contacts is regarded as typical for chlorinated aromatic hydrocarbons that are characterized by low C–Cl bond polarity (C–Cl distance of about 1.70–1.73 Å) and rather rare in the case of highly polar C–Cl bonds with C–Cl distances of 1.79–1.81 Å. Taking into account the enormous extension of C–Cl bond lengths in the presented $C_{78}Cl_{18}$ molecules (1.84–1.87 Å), which should lead to localization of a significant negative charge on the Cl atoms, the participation of these Cl atoms in short Cl···Cl contacts is largely unexpected. However, analyses of the respective crystal structures of halogenated C_{78}(2–4) fullerenes, clearly point to the presence of attractive intermolecular Cl···Cl interactions, the nature of which is presumably different from that of the halogen bonding described previously.

Results and Discussion

$C_{78}(4)Cl_{18}$ forms solvent-free crystals in the hexagonal space group $P6_3/m$. The quality of the crystals obtained has granted an accurate structure determination presenting all atoms in ordered and fixed positions.[9] $C_{78}(3)Cl_{18}$ is displaying the same overall packing as $C_{78}(4)Cl_{18}$, but the fullerene molecules are disordered between three orientations. $C_{78}(2)Cl_{18}$ crystallizes in the hexagonal space group $P6_3/mmc$ and is as well characterized by fullerene disorder around the threefold crystallographic axis. Despite the statistical disorder in structures **I** and **II**, the connectivities of both isomers can be reliably derived from X-ray data. Both isomers $C_{78}(2)Cl_{18}$ and $C_{78}(3)Cl_{18}$, and the pristine $C_{78}(2)$ and $C_{78}(3)$, possess C_{2v} point-group symmetry and differ formally in the orientation of only one C–C bond. Virtually, both fullerene molecules can be represented as a combination of two trimethyltrindane fragments, capping the cage from the top and bottom, with three pyracylene fragments encircling it (Figure 1). In the case of $C_{78}(2)$, two of the three pyracylene fragments are disposed in such a manner that the central C–C bond is perpendicular to the equatorial mirror plane, whereas in the third one this bond is parallel to the same plane. For $C_{78}(3)$, the situation is reversed. In both crystal structures (**I** and **II**), the fullerene molecules are orientationally disordered around the threefold axis. Since the symmetry of both fullerene derivatives approaches D_{3h}, the position of all carbon atoms except those forming the central bond in the pyracylene unit virtually superimpose under 120° rotation. As a consequence, the obtained disorder does not obstruct the reliable structure determination because the isomer's identity is unambiguously given by the relative site occupancies of the carbon atoms constituting the central bond in the pyracylene subunit.

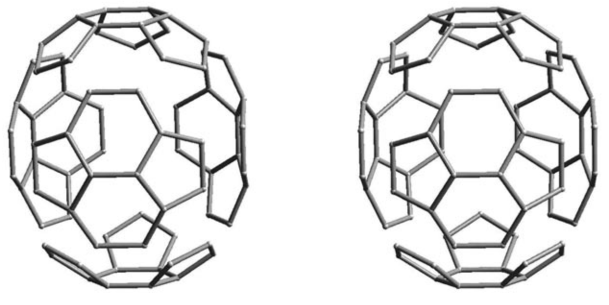

Figure 1. Stereoview of $C_{78}(2)$ showing the partitioning of the fullerene cage into two trimethyltrindane (methyl groups are omitted for clarity) and three pyracylene fragments.

Analysis of crystal structure **I** gives the site occupancies of the carbon atoms constituting the parallel and perpendicular—relative to the equatorial mirror plane—central bonds in the pyracylene subunits of 0.65:0.35, respectively, which assigns the structure to the $C_{78}(3)$ isomer (expected site occupancies of 0.67:0.33). The experimental site occupancies of 0.36:0.64 in crystal structure **II** attribute it to the $C_{78}(2)$ isomer (theoretically 0.33:0.67).

By superimposing DFT-optimized $C_{78}Cl_{18}$ structure models, disorder around the threefold axis has been simulated. As can be seen from Figure 2, remarkable deviation from D_{3h} symmetry is observed only for the equatorial pyracylene fragments. Comparing the superposition of three orientations of the calculated structure with the results of X-ray data refinement of $C_{78}(3)Cl_{18}$ reveals that only the carbon atoms constituting the pyracylene fragments display some prolongation of the experimentally obtained thermal ellipsoids (see Figure 2, right), whereas the rest of the carbon as well as the chlorine atoms are more symmetrical with respect to the shape of their displacement ellipsoids, which is in a good agreement with the presented model. It is worth mentioning that chlorine atoms follow the partitioning of the carbon cage into chlorine-substituted trimethyltrindane and pyracylene fragments, resulting in a tiny enlargement of the displacement ellipsoids of chlorine atoms attached to the pyracylene entity (for further reference see Figure S1 in the Supporting Information). Thus, in the case of $C_{78}(2)Cl_{18}$ and $C_{78}(3)Cl_{18}$, not only the molecular structure can be reliably determined, but also some bond distances in-

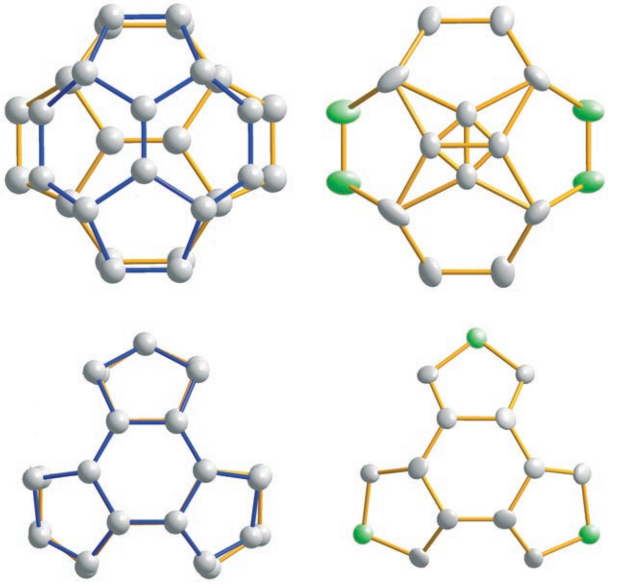

Figure 2. Left: superposition of all three orientations of the pyracylene (top) and trindane fragments (bottom) from the DFT-derived model of $C_{78}(3)Cl_{18}$. The blue bonding pattern represents the two coinciding fragments, whereas the orange pattern depicts the third. Right: ORTEP plots of corresponding fragments in the crystal structure of $C_{78}(3)Cl_{18}$. Chlorine bearing carbon atoms are presented in green.

cluding intermolecular Cl···Cl contacts can be assessed with satisfying accuracy.

The chlorination patterns of $C_{78}(2)Cl_{18}$, $C_{78}(3)Cl_{18}$, and $C_{78}(4)Cl_{18}$ are presented in Figure 3. The difference between these structures is formally in the position of the equatorial double bonds. The stabilizing factor of the localization of chlorine atoms is the formation of nine close-to-planar aromatic C–C rings and the absence of double bonds in the pentagons, which is typical for halogenated fullerenes.[2k]

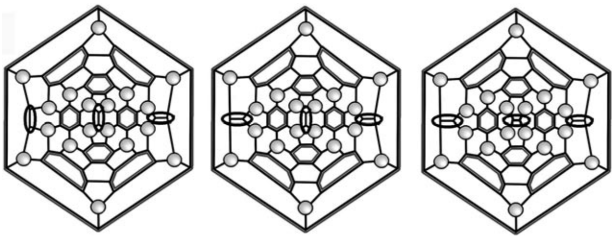

Figure 3. Schlegel diagram of $C_{78}(2)Cl_{18}$ (left), $C_{78}(3)Cl_{18}$ (center), and $C_{78}(4)Cl_{18}$ (right). The aromatic zones are double-marked and the chlorine atoms are depicted by spheres. The difference between the structures lies in the orientation of the equatorial C–C bonds (selected).

It has generally been assumed that the elongation of a C–Cl covalent bond leads to localization of negative charge on the Cl atom. The C–Cl bonds in all $C_{78}Cl_{18}$ molecules are strongly elongated (1.84–1.88 Å). According to an empirical approach to the estimation of bond orders,[16] the order of C–Cl bonds with lengths of about 1.87 Å is only 0.65, which should lead to a very high degree of polarity of these bonds and consequently to localization of significant negative charge on the Cl atom. However, within the crystal packing of $C_{78}(3)Cl_{18}$ and $C_{78}(4)Cl_{18}$, the chlorine atoms form an extensive 3D Cl···Cl network with short intermolecular Cl···Cl separations, which challenge the concept of "high polarity" of C–Cl bonds. Since within the crystal of $C_{78}(3)Cl_{18}$ and $C_{78}(4)Cl_{18}$ all 18 chlorine atoms are engaged in the formation of Cl···Cl contacts, and all of these are short, the responsible forces have to be inevitably attributed to some attractive interactions between chlorine atoms. It is important to mention that there are no other intermolecular contacts besides Cl···Cl, which could "squeeze" the atoms together, thus influencing the molecular packing. Thus, both crystal structures appear to provide unambiguous evidence for the attractive nature of these intermolecular interactions, and challenge at the same time all explanations given so far, discussing this kind of "bonding".

A closer look at the structure in Figure 4 reveals the presence of two- as well as three-centered contacts between the chlorine atoms. The existence of such three-centered contacts prompts each $C_{78}Cl_{18}$ molecule to form 24 short Cl···Cl separations, all of about 3.34–3.45 Å. Thus, even if the distance of 3.45 Å in the two-centered contacts (structure **III**) could be attributed to the close packing of anisotropic chlorine atoms, the distances of 3.38 (structure **I**) and 3.34 Å (structure **III**) in the three-centered contacts are inexplicable in terms of this model. Additional confirmation of the attractive nature of Cl···Cl interactions can be obtained considering two- and three-centered Cl···Cl contacts in $C_{78}(4)Cl_{18}$. In this case, structurally equal C–Cl bonds (according to the inherent D_{3h} point-group symmetry of $C_{78}(4)Cl_{18}$) are involved in both types of interactions. It was found that in the case of the three-centered Cl···Cl contacts, the respective C–Cl bonds are elongated (1.862(11) Å) in

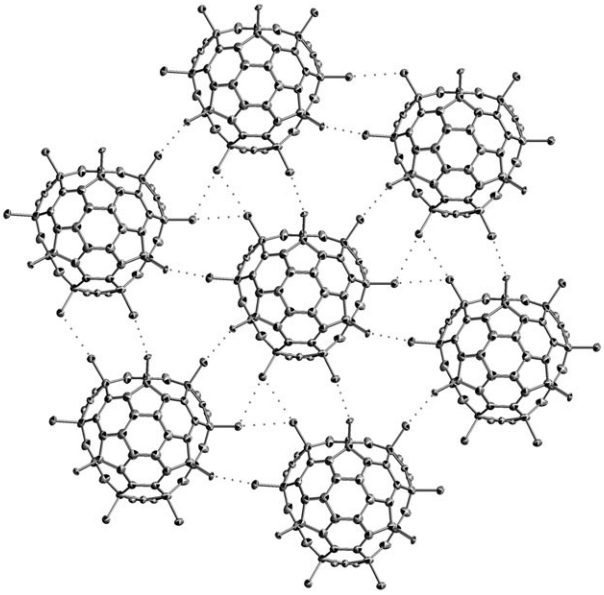

Figure 4. ORTEP projection of $C_{78}(3)Cl_{18}$ showing short two- and three-centered Cl···Cl contacts (represented by •••••).

comparison to those in which two-centered contacts are formed (1.829(11) Å). Moreover, the intermolecular Cl···Cl distances of 3.34 Å in the three-centered contacts are shorter than those in the two-centered (3.45 Å). Such elongation of the C–Cl bonds involved in the shorter Cl···Cl separations, regions in which negative charge accumulation would have generated a strong repulsive force, can only be explained by the attractive nature of the interactions between chlorine atoms.

The first example of an unusually short intermolecular Cl···Cl contact (3.21 Å) between two "highly polar" Cl atoms was reported more than 20 years ago in the crystal structure of triphenylmethane chloride.[17] To our knowledge, no other crystal structures of chlorinated hydrocarbons with such short Cl···Cl separations between chlorine atoms involved in highly elongated C–Cl bonds (above 1.85 Å) have ever been reported. Recently, we have found that the chlorine atoms in the structure of $C_{76}Cl_{18}$ form a number of extremely short Cl···Cl contacts of about 3.14–3.21 Å,[3] which are about 0.45 Å shorter than the sum of the van der Waals radii. As a very interesting and important fact, all four elongated C–Cl bonds (1.821(1)–1.850(1) Å) are involved in such contacts, whereas ten "usual" C–Cl bonds with lengths of 1.777(1)–1.797(1) Å do not form any short Cl···Cl contacts. Some chlorinated C_{60} fullerenes—$C_{60}Cl_{28}$[2d] and $C_{60}Cl_{30}$[2j]—also form short Cl···Cl contacts, although the C–Cl bonds in these structures are not strongly elongated (1.78–1.80 Å). The structural similarity of the chlorine-bearing fragments in triphenylmethane chloride,[17] $C_{76}Cl_{18}$,[3] and the present $C_{78}Cl_{18}$ molecules leads toward the assumption that the tendency of forming short Cl···Cl contacts is due to the unique bonding characteristics of carbon rather than the nature of the chlorine atom itself. In all mentioned cases, the corresponding chlorine atoms are connected to sp^3-hybridized carbon atoms, which in turn are directly connected to three phenyl rings. The angular symmetry at the sp^3 carbon atom is considerably distorted from tetrahedral. Obviously, such geometry results in a partial rehybridization of the corresponding carbon atom that assumes additional sp^2 character. The three neighboring aromatic rings additionally stabilize this configuration since the molecule adopts a more extended aromatic state. As a result of the reduced overlap efficiency between chlorine and carbon atom orbitals, the corresponding C–Cl bonds are significantly elongated. Consequently, the short intermolecular distances between these chlorine atoms indicate that C–Cl bonds cannot be regarded as highly polar, and significant localization of negative charge on the chlorine atom is less probable. Thus, the elongation of the C–Cl bonds and the absence of strong negative charge on the Cl atoms leads to the assumption that the corresponding covalent bonds are partially homolytically dissociated. This model would consistently explain all the features discussed. The partial homolytic cleavage of C–Cl bonds will impart a partial radical character to the chlorine atoms, which breaks up the closed-shell character of chlorine and enables it to undergo some weak intermolecular bonding.

Within the crystal packing of $C_{78}(2)Cl_{18}$, each molecule forms 12 Cl···Cl contacts with distances of about 3.39 Å (Figure 5). Such an orientation in the crystal leads to the formation of two dissimilarly sized voids: the larger ones contain disordered $TiCl_4$ molecules, whereas the smaller ones are occupied by Br_2 molecules. The bromine molecule is disordered between six equivalent positions, each oriented along the axis connecting two chlorine atoms as shown in Figure 6. As can be concluded from the electron-density map (see the Supporting Information), the bromine molecule is fixed between two chlorine atoms (Figure 6). The Cl···Br distance of 3.21 Å is enormously short (the sum of the van der Waals radii is 3.6–3.7 Å). The fact that the Br_2 molecule is oriented between two chlorine atoms rather than avoiding any short interhalogen contacts, regardless of the abundant space available (see Figure 6, right), as well as the rigidity of the "molecular box" in which it is imprisoned,

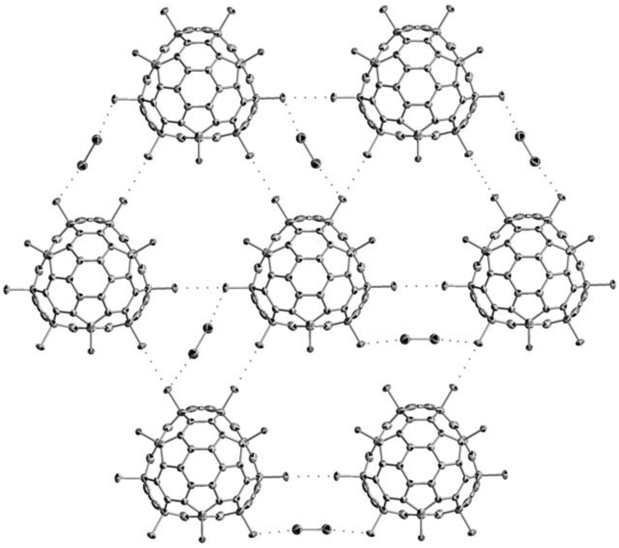

Figure 5. ORTEP projection of $C_{78}(2)Cl_{18}{\cdot}Br_2{\cdot}TiCl_4$ in the crystal. $TiCl_4$ is omitted for clarity. Only one orientation of the Br_2 molecule is presented. Short contacts are depicted by •••••.

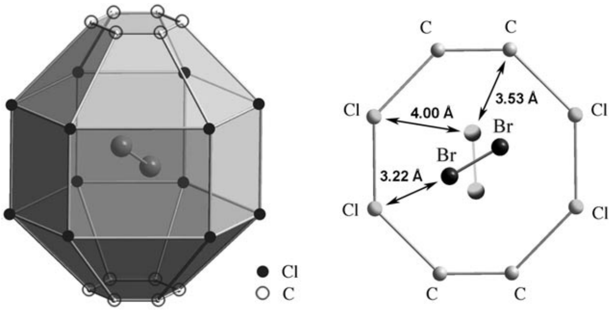

Figure 6. Left: Br_2 in the "molecular box" Right: the orientation and relative distances between chlorine atoms and the bromine molecule according to the X-ray experiment (depicted in black) and the orientation of Br_2 representing minimized interhalogen repulsions (depicted in gray).

thus diminishing the influence of crystal-packing forces, confirms the attractive nature of halogen–halogen interactions in the given system. The angle C-Cl···Br is close to 120°, which represents an energetically unfavorable geometry for a close-contact formation according to quantum-chemical calculations.[13] In the case of Cl···Cl contacts, such an orientation results in an exchange-repulsion energy of about 5 kcal mol^{-1},[13] and is expected to be even higher in the case of Cl···Br contacts. It is easy to assume that the attractive forces should be higher than 5 kcal mol^{-1}, and notwithstanding that such halogen–halogen "bonding" can be classified as weak, the cumulative effect can constitute significant values of energy. For example, in the case of $C_{78}(3)Cl_{18}$ and $C_{78}(4)Cl_{18}$, the formation of 24 such "bonds" can provide an amount of energy equal to about 120 kcal mol^{-1}, which is higher than the energy of a single C–C bond.

Experimental Section

Preparation of $C_{78}(2)Cl_{18}$, $C_{78}(3)Cl_{18}$, and $C_{78}(4)Cl_{18}$: The pristine C_{78} fullerene isomers—$C_{78}(2)$, $C_{78}(3)$, and $C_{78}(4)$—were produced by evaporation of graphite along the RF-furnace route, details of which have been reported elsewhere.[18] Collected soot was soxhlet extracted with CS_2 and separated by three-step HPLC. Prior to separation, CS_2 was substituted for toluene. For the first step of separation (fraction collection), a Buckyprep column 20×250 mm was used. The second step, recycling HPLC, was executed with a Buckyprep column 10×250 mm aiming at the separation of the two main subfractions: the first one containing a mixture of $C_{78}(1)$ and $C_{78}(2)$ fullerenes and the second one pure $C_{78}(3)$. Toluene was used as a mobile phase for the first and second steps of separation with flow rates of 20 and 5 mL min^{-1}, respectively. The final step of isolation was performed with a $5C_{18}$-AR-II column 10×250 mm rendering chromatographically pure $C_{78}(2)$ fullerene in five consecutive cycles. The composition of the mobile phase was adjusted to 45 v/v% acetonitrile in toluene, with a flow rate of 5 mL min^{-1}. The isolation and chlorination of $C_{78}(4)$ were reported previously.[9] The new fullerene halides were obtained through chlorination of the pristine fullerenes (0.5 mg each) in a mixture of $Br_2/TiCl_4$ (1.5 mL, 1:100 v/v) in glass ampoules. The ampoules were cooled with liquid nitrogen, evacuated, and sealed. Yellow crystals in the case of $C_{78}(3)$ and $C_{78}(4)$, and red crystals in the case of $C_{78}(2)$ formed directly on the glass wall after keeping the mixture at 100 °C for one week. Subsequently, the ampoules were cut open and the excess solvent decanted. The products were found to be stable in air for at least one month.

Crystal data: X-ray diffraction data were obtained by using a Bruker APEX II CCD difractometer ($Mo_{K\alpha}$ radiation ($\lambda = 0.71073$ Å), graphite monochromator). The crystal structures were solved and all atoms refined in the anisotropic approximation by using SHELTXL.[19]

*Crystal data for structure **I**, $C_{78}(3)Cl_{18}$*: Yellow crystal, 0.04×0.02×0.01 mm; hexagonal; space group = $P6_3/m$; $a = 13.0202(16)$, $c = 18.726(5)$ Å; $V = 2749.3(8)$ Å^3; $Z = 2$; $2\theta_{max} = 42.0°$; $-13 < h < 13$, $-13 < k < 13$, $-18 < l < 18$; $T = 100(2)$ K; data/restraints/parameters = 1025/0/147; $\mu = 0.953$ mm^{-1} (transmission min/max = 0.977/0.991); final R value = 0.0434 ($R_w = 0.1316$).

*Crystal data for structure **II**, $C_{78}(2)Cl_{18}\cdot Br_2\cdot TiCl_4$*: Red crystal, 0.02×0.01×0.01 mm; hexagonal; space group = $P6_3/mmc$; $a = 14.6910(13)$, $c = 17.045(2)$ Å; $V = 3186.0(6)$ Å^3; $Z = 2$; $2\theta_{max} = 45.0°$; $-15 < h < 15$, $-15 < k < 15$, $-18 < l < 18$; $T = 100(2)$ K; data/restraints/parameters = 826/7/114; $\mu = 2.365$ mm^{-1} (transmission min/max = 0.954/0.976); final R value = 0.0711 ($R_w = 0.2234$).

*Crystal data for structure **III**, $C_{78}(4)Cl_{18}$*: Yellow crystal, 0.02×0.02×0.01 mm; hexagonal; space group = $P6_3/m$; $a = 13.055(5)$, $c = 18.762(14)$ Å; $V = 2769(2)$ Å^3, $Z = 2$; $2\theta_{max} = 41.74°$; $-13 < h < 13$, $-13 < k < 13$, $-18 < l < 18$; $T = 100(2)$ K; data/restraints/parameters = 1018/0/118; $\mu = 0.946$ mm^{-1} (transmission min/max = 0.964/0.988); final R value = 0.0601 ($R_w = 0.1629$).

CCDC-662360 (structure **I**, $C_{78}(3)Cl_{18}$), 653031 (structure **II**, $C_{78}(2)Cl_{18}\cdot Br_2\cdot TiCl_4$), and 686048 (structure **III**, $C_{78}(4)Cl_{18}$) contain the supplementary crystallographic data for this paper. These data can be obtained free of charge from The Cambridge Crystallographic Data Centre via www.ccdc.cam.ac.uk/data_request/cif

Computations: Quantum-chemical calculations were performed by using the density-functional method of B3LYP/6-31G with Gaussian 03.[20]

Acknowledgement

We gratefully acknowledge generous support by the Fonds der Chemischen Industrie, and thank to Dr. J. Nuss for collecting the X-ray data.

---

[1] I. S. Neretin, Y. L. Slovokhotov, *Russ. Chem. Rev.* **2004**, *73*, 455–486.

[2] a) P. R. Birkett, P. B. Hitchcock, H. W. Kroto, R. Taylor, D. M. Walton, *Nature* **1992**, *357*, 479–481; b) F. N. Tebbe, R. L. Harlow, D. B. Chase, D. L. Thorn, G. C. Campbell, J. C. Calabrese, N. Herron, R. J. Young, E. Wasserman, *Science* **1992**, *256*, 822–825; c) P. A. Troshin, R. N. Lyubovskaya, I. N. Ioffe, N. B. Shustova, E. Kemnitz, S. I. Troyanov, *Angew. Chem.* **2005**, *117*, 238–241; *Angew. Chem. Int. Ed.* **2005**, *44*, 234–237; d) S. I. Troyanov, N. B. Shustova, A. A. Popov, L. N. Sidorov, E. Kemnitz, *Angew. Chem.* **2005**, *117*, 436–439; *Angew. Chem. Int. Ed.* **2005**, *44*, 432–435; e) S. I. Troyanov, A. A. Popov, *Angew. Chem.* **2005**, *117*, 4287–4290; *Angew. Chem. Int. Ed.* **2005**, *44*, 4215–4218; f) N. B. Shustova, A. A. Popov, L. N. Sidorov, A. P. Turnbull, E. Kemnitz, S. I. Troyanov, *Chem. Commun.* **2005**, 1411–1413; g) S. I. Troyanov, N. B. Shustova, I. N. Ioffe, A. P. Turnbull, E. Kemnitz, *Chem. Commun.* **2005**, 72–74; h) P. R. Birkett, A. G. Avent, A. D. Darwish, H. W. Kroto, R. Taylor, D. R. Walton, *J. Chem. Soc. Chem. Commun.* **1995**, *6*, 683–684; i) S. I. Troyanov, A. A. Popov, N. I. Denisenko, O. V. Boltalina, L. N. Sidorov, E. Kemnitz, *Angew. Chem.* **2003**, *115*, 2497–2500; *Angew. Chem. Int. Ed.* **2003**, *42*, 2395–2398; j) S. I. Troyanov, N. B. Shustova, A. A. Popov, L. N. Sidorov, *Russ. Chem. Bull.* **2005**, *54*, 1656–1666; k) S. I. Troyanov, E. Kemnitz, *Eur. J. Org. Chem.* **2005**, *23*, 4951–4962.

[3] K. S. Simeonov, K. Y. Amsharov, M. Jansen, *Angew. Chem.* **2007**, *119*, 8571–8573; *Angew. Chem. Int. Ed.* **2007**, *46*, 8419–8421.

[4] P. W. Fowler, D. E. Manolopoulous, *An Atlas of Fullerenes*, Clarendon, Oxford, **1995**.

[5] F. Diederich, R. L. Whetten, C. Thilgen, R. Ettl, I. Chao, M. M. Alvarez, *Science* **1991**, *254*, 1768–1770.

[6] T. Wakabayashi, K. Kikuchi, S. Suzuki, H. Shiromaru, Y. Achiba, *J. Phys. Chem.* **1994**, *98*, 3090–3091.

[7] a) S. I. Troyanov, E. Kemnitz, *Eur. J. Org. Chem.* **2003**, *20*, 3916–3919; b) A. V. Burtsev, E. Kemnitz, S. I. Troyanov, *Crystallogr. Rep.* **2008**, *53*, 639–644.

[8] N. B. Shustova, B. S. Newell, S. M. Miller, O. P. Anderson, R. D. Bolskar, K. Seppelt, A. A. Popov, O. V. Boltalina, S. H. Strauss, *Angew. Chem.* **2007**, *119*, 4189–4192; *Angew. Chem. Int. Ed.* **2007**, *46*, 4111–4114.

[9] K. S. Simeonov, K. Y. Amsharov, E. Krokos, M. Jansen, *Angew. Chem.* **2008**, *120*, 6379–6381; *Angew. Chem. Int. Ed.* **2008**, *47*, 6283–6285.

[10] O. V. Grineva, P. M. Zorky, *Crystallogr. Rep.* **2000**, *45*, 633–639.

[11] a) G. R. Desiraju, R. Parthasarathy, *J. Am. Chem. Soc.* **1989**, *111*, 8725–8726; b) N. Ramasubbu, R. Parthasarathy, P. Murray-Rust, *J. Am. Chem. Soc.* **1986**, *108*, 4308–4314; c) T. Sakurai, M. Sundaralingam, G. A. Jeffrey, *Acta Crystallogr.* **1963**, *16*, 354–363.

[12] S. C. Nyburg, C. H. Faerman, *Acta Crystallogr. Sect. B* **1985**, *41*, 274–279.

[13] S. L. Price, A. J. Stone, J. Lucas, R. S. Rowland, A. E. Thornley, *J. Am. Chem. Soc.* **1994**, *116*, 4910–4918.

[14] a) P. Politzer, P. Lane, M. C. Concha, Y. Ma, J. S. Murray, *J. Mol. Model.* **2007**, *13*, 305–311; b) A. K. Brisdon, *Annu. Rep. Prog. Chem. Sect. A* **2005**, *101*, 128–138; c) P. Metrangolo, H. Neukirch, T. Pilati, G. Resnati, *Acc. Chem. Res.* **2005**, *38*, 386–395; d) M. Fourmigue, P. Batail, *Chem. Rev.* **2004**, *104*, 5379–5418. e) C. Ouvrard, J. Y. Le Questel, M. Berthelot, C. Laurence, *Acta Crystallogr. Sect. B* **2003**, *59*, 512–526.

[15] J. P. M. Lommerse, A. J. Stone, R. Taylor, F. H. Allen, *J. Am. Chem. Soc.* **1996**, *118*, 3108–3116.

[16] a) G. Lendvay, *J. Mol. Struct.* **2000**, *501–502*, 389–393; b) J. P. Paolini, *J. Comput. Chem.* **1990**, *11*, 1160–1163. c) T. Anno, A. Sado, *J. Chem. Phys.* **1956**, *25*, 176–177.

[17] A. Dunand, R. Gerdil, *Acta Crystallogr. Sect. B* **1982**, *38*, 570–575.

[18] a) M. Jansen, G. Peters, N. Wagner, *Z. Anorg. Allg. Chem.* **1995**, *621*, 689–693; b) G. Peters, M. Jansen, *Angew. Chem.* **1992**, *104*, 240–242; *Angew. Chem. Int. Ed. Engl.* **1992**, *31*, 223–224.

[19] G. M. Sheldrick, SHELXTL DOS/Windows/NT, Version 6.14; Bruker Analytical X-Ray Instruments, Inc., Madison, WI, **1997**.

[20] Gaussian 03 (Revision C 02), M. J. Frisch, G. W. Trucks, H. B. Schlegel, G. E. Scuseria, M. A. Robb, J. R. Cheeseman, J. A. Montgomery, Jr., T. Vreven, K. N. Kudin, J. C. Burant, J. M. Millam, S. S. Iyengar, J. Tomasi, V. Barone, B. Mennucci, M. Cossi, G. Scalmani, N. Rega, G. A. Petersson, H. Nakatsuji, M. Hada, M. Ehara, K. Toyota, R. Fukuda, J. Hasegawa, M. Ishida, T. Nakajima, Y. Honda, O. Kitao, H. Nakai, M. Klene, X. Li, J. E. Knox, H. P. Hratchian, J. B. Cross, V. Bakken, C. Adamo, J. Jaramillo, R. Gomperts, R. E. Stratmann, O. Yazyev, A. J. Austin, R. Cammi, C. Pomelli, J. W. Ochterski, P. Y. Ayala, K. Morokuma, G. A. Voth, P. Salvador, J. J. Dannenberg, V. G. Zakrzewski, S. Dapprich, A. D. Daniels, M. C. Strain, O. Farkas, D. K. Malick, A. D. Rabuck, K. Raghavachari, J. B. Foresman, J. V. Ortiz, Q. Cui, A. G. Baboul, S. Clifford, J. Cioslowski, B. B. Stefanov, G. Liu, A. Liashenko, P. Piskorz, I. Komaromi, R. L. Martin, D. J. Fox, T. Keith, M. A. Al-Laham, C. Y. Peng, A. Nanayakkara, M. Challacombe, P. M. W. Gill, B. Johnson, W. Chen, M. W. Wong, C. Gonzalez, J. A. Pople, Gaussian, Inc., Wallingford, CT, **2004**.

Received: June 17, 2008